Alexandria Engineering Journal (2018) 57, 1657–1664

Alexandria University

Alexandria Engineering Journal

www.elsevier.com/locate/aej
www.sciencedirect.com

ORIGINAL ARTICLE

Study on reducibility and porosity of metallurgical sinter

Simona Jursova [a,*], **Pavlina Pustejovska** [a], **Silvie Brozova** [b]

[a] *VŠB – Technical University of Ostrava, Centre ENET, 17. listopadu 15, 708 33 Ostrava – Poruba, Czech Republic*
[b] *VŠB – Technical University of Ostrava, Faculty of Metallurgy and Material Engineering, 17. listopadu 15, 708 33 Ostrava – Poruba, Czech Republic*

Received 6 April 2016; revised 14 February 2017; accepted 4 March 2017
Available online 25 March 2017

KEYWORDS

Sinter;
Reduction;
Porosity;
Density;
Structure

Abstract The paper dealt with research on structural properties of metallurgical sinter. It was aimed at studying of sinter porosity and density in relation to its reducibility. For porosity determination was used immersion technique using Archimedes principle. Density was measured by gas pycnometer and apparent density was calculated from results of measured porosity. These properties were studied in relation to temperature 950 °C at which reducibility tests of every sample were carried out according to ISO 4695:2007. For the study 7 batches of 5 samples of sinter originated from industrial metallurgical plant were sorted. The porosity and density were discussed for virgin samples before the test of reducibility and for reduced samples after ISO test. The effect of 950 °C on the properties was contemplated and SEM analysis was carried out. The samples porosity before reduction test was in range from 5.1% to 9.82% and for the samples after reduction test it was 32.77–44.12%. The density of samples was not significantly affected by temperature with values ranging from 3.65 to 3.82 g cm^{-3} for virgin samples, resp. 4.87–5.37 g cm^{-3} for samples after reduction.

1. Introduction

Sintered iron ores are consumed by most of the modern blast furnaces as the iron feed to the blast furnace feedstock [1]. The formation of the sinter structure is highly complex process accompanied by a large number of factors related to the process technology as well as chemical and physical phenomena during the sintering process. For optimal processing of sinter in blast furnaces, the knowledge on sinter structure and sinter reducibility is essential. The mineralogical structure, porosity of sintered materials and its formation have been widely studied. Nishioka revealed that the pore sizes have a great influence on the effective thermal diffusivity as well as porosity [2]. McCann et al. discussed the specific heat capacity as well as chemical and structural changes of iron ores during its heating [3]. The attention was also paid to the statistical geometric characteristics of the pore structure. Aizawa and Suwa worked out a mathematical model to define effects of porosity, pore size, shape and their distribution [4]. Fröhlichova et al. analyzed the sinter structure in view of titanium addition to it [5]. Tian et al. reported a characterization of sinter on its

* Corresponding author.
E-mail addresses: simona.jursova@vsb.cz (S. Jursova), pavlina.pustejovska@vsb.cz (P. Pustejovska), silvie.brozova@vsb.cz (S. Brozova).
Peer review under responsibility of Faculty of Engineering, Alexandria University.

http://dx.doi.org/10.1016/j.aej.2017.03.007

structural and thermophysical properties toward waste heat recovery applications. They used a fractal model to predict the effective thermal conductivity as a function of porosity [6]. Bölükbaşi et al. studied porosity and structure of metallurgical sinter in relation to its quality [7].

Various measurement techniques were applied for sinter structure characterization. By Janowski et al. the stereologic analysis of a solid grain of reduced hematite was applied for determination of its porosity [8]. Shatokha et al. analyzed sinter porosity by application of 3D tomography method [9,10]. A mention about morphological investigation and reducibility testing used for lump ores brand characterization in industrial – scale process conditions was presented in a research paper by Hanel et al. [11].

However, studies about relation between structural properties such as porosity and reducibility are not numerous and are associated with great uncertainties due to the variations in the structure and composition of sinter. This paper wanted to present results of research on porosity and density of metallurgical sinter originated from a European metallurgical plant in a view of sinter reducibility. For porosity determination was applied a simple technique accessible for research institutions with no need of significant investments. The purpose of this paper was to deepen general understanding of structure metallurgical sinter. The results were intended to contribute to general knowledge about correlation between sinter structure and its reducibility. In the paper were presented first results of research on comprehensive structural analysis such as porosity and density. Evaluation of the acquired results was intended for following research on pore distribution, pore sizes and shape and specific surface area of accessible pores.

Generally, the best metallurgical properties are contemplated in sinter with pores less than 4 mm equally dispersed in the material [12,13]. Sinter with unequally dispersed big pores is hardly reducible and little strong. The most strong is that one that has monolith stone structure, and on the other hand its reducibility is very low and processing of this kind of sinter is typical of high fuel consumption [14]. The sinter porosity is decreased by increasing fuel consumption, decreasing ratio of return sinter and decreasing sinter basicity [15].

2. Experimental procedure

Experimental work was done on seven samples of metallurgical sinter from the production of a Czech metallurgical company. The samples were marked in Figs. 1–7 according to the order of their processing. Chemical composition of the tested material is shown in Tables 1 and 2.

2.1. Reducibility determination

Tests of sinters reducibility dR/dt (%/min) were conducted according to ISO 4695:2007. The samples of size range 10.0–12.5 mm were oven-dried to constant mass at 105 °C ± 5 °C and before preparation of the test portions they were cooled to room temperature. The test portion of 500 g was isothermally reduced at 950 °C in a fixed bed of reduction tube with a removable perforated plate inside ensuring uniform gas flow using reducing gas consisting 40.0% of CO and 60.0% of N_2

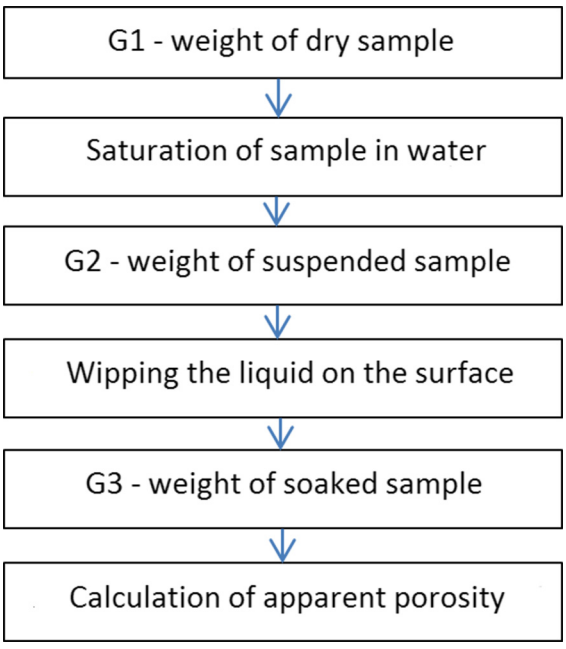

Figure 1 Scheme of porosity measuring.

[15]. The portion was weighed at specified time intervals until its degree of reduction reaches 65%. The degree of reduction R_t, relative to the iron (III) state after t min is calculated, as follows (1) [16].

$$R_t = \left(\frac{0.111 w_1}{0.430 w_2} + \frac{m_1 - m_t}{m_0 \cdot 0.430 w_2} \cdot 100\right) \cdot 100 \quad (1)$$

Where

m_0 is the start mass of the test portion before heating to reduction temperature 950 °C [g]
m_1 is the mass of the portion heated for 950 °C and immediately before starting the reduction [g]
m_t is the mass of the test portion after reduction time t [g]
w_1 is the iron (II) oxide content [%]
w_2 is the total iron content [%]

The reducibility index, expressed as the rate of reduction at the atomic ratio of O/Fe of 0.9 [%/min] is calculated from Eq. (2) and is presented in Table 3.

$$\frac{dR}{dt}\left(\frac{O}{Fe} = 0.9\right) = \frac{33.6}{t_{60} - t_{30}} \quad (2)$$

where

t_{30} is the time to attain a degree of reduction of 30% [min]
t_{60} is the time to attain a degree of reduction of 60% [min]

2.2. Porosity determination

Porosity of the tested sinters ϕ (%) was determined by immersion method applying Archimedes principle as the buoyant force on a submerged object is equal to the weight of the fluid that is displaced by the object. The procedure of porosity measuring is presented in Fig. 1.

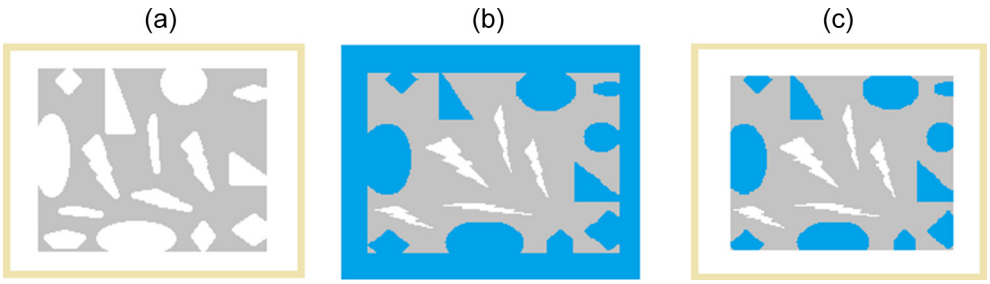

Figure 2 Definition of samples during porosity measuring.

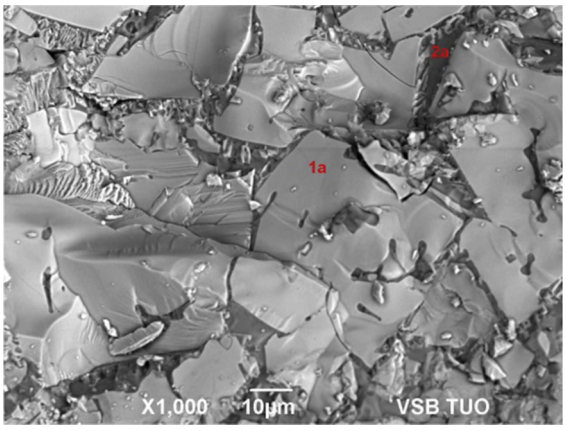

Figure 3 Surface of sample 2 before reduction.

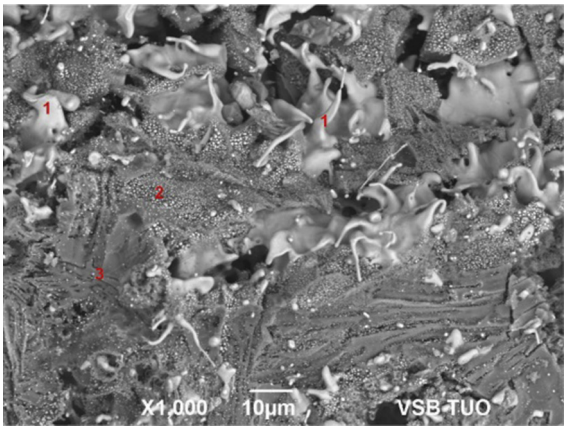

Figure 5 Surface of sample 2 after reduction.

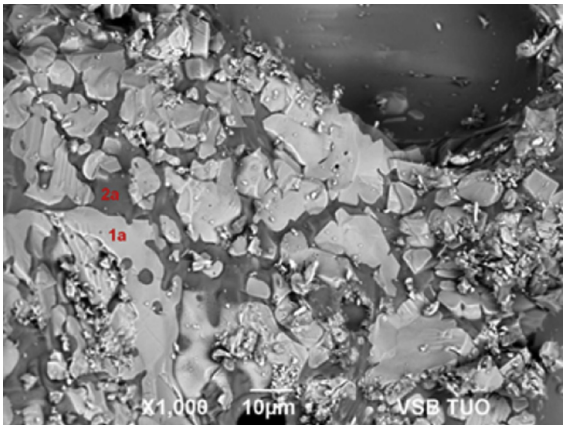

Figure 4 Surface of sample 3 before reduction.

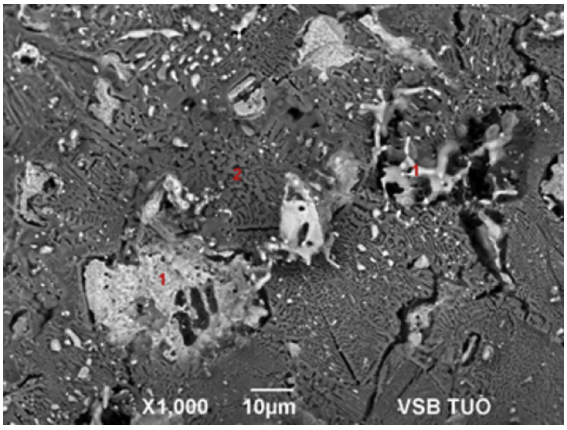

Figure 6 Surface of sample 3 after reduction.

For the final porosity calculation dry weights (a), suspended weights of samples (b) and soaked weights of samples (c) (Fig. 2) were used according to Eq. (1).

$$\Phi[\%] = \frac{G_3 - G_1}{G_3 - G_2} \cdot 100 \quad (3)$$

where

G_1 dry weight [g]
G_2 suspended weight [g]
G_3 soaked weight [g]

For each type of tested sinters, five samples were taken to determine their porosity. The average porosity of sinters samples is summarized in Tables 4 and 5. They present porosity of virgin samples and porosity of samples after the test of reducibility.

2.3. Density determination

The apparent density ρ (g/cm^3) and the true density of the solid matrix ρ_s (g/cm^3) were determined. The true density of samples was determined using gas pycnometer Accupyc 1330, whereas the apparent one was calculated using data acquired during porosity measurements following Archimedes principles, as follows (4):

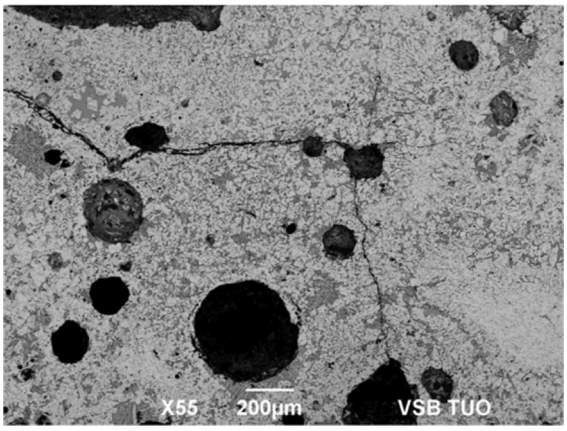

Figure 7 SEM on sample 2 before reduction.

$$\rho_Z = \rho_{H_2O} \frac{G_1}{G_3 - G_2} \quad (4)$$

where

ρ_{H_2O} density of water 998 kg m^{-3}

The results of density measuring are presented in Tables 4 and 5.

3. Results and discussion

The reducibility of tested samples reached values lower than 1%·min^{-1} excluding highly basic sample 2. In compliance with many research [16–20] it confirmed positive effect of higher basicity on sinter reducibility. However, reducibility index of sample 1 with higher basicity is noticeably low which relates to high FeO content. Results of porosity measurements proved the strong effect of high temperature on pores volume. It was noted that the porosity, as measured by the water displacement method, represented the porosity of closed-pores, ranging from 5.1% to 9.82% for virgin samples before reduction and much higher values for samples after reduction at 950 °C in range from 32.77% to 44.12%. The porosity of presented virgin samples is lower than it was mentioned in the literature [6] with average porosity ranging from 12% to 24%. However, density of samples was affected by high temperature just slightly. High temperature of reducibility tests increased the density around 1 g cm^{-3}. The apparent density in range from 3.65 to 3.82 g cm^{-3} responded the experience [6].

The most porous sample was sample 2 with FeO content 7.00% and extremely high basicity 2.33. In accordance with worldwide experience [21], this sample was very well reducible. High reduction index relates to sample properties such as its high basicity and its high porosity. Metallurgical sinter with low basicity has a high ratio of fayalite which affects sintering process with extremely high generation of liquid phase making

Table 3 Reducibility of samples.

Sample	dR/dt [%·min^{-1}]	Basicity
1	0.53	1.70
2	1.31	2.33
3	0.81	1.22
4	0.65	0.99
5	0.71	1.80
6	0.89	0.87
7	0.70	0.98

Table 1 Chemical analysis of tested sinters – Part 1.

Sample	FeO	Fe	C	Mn	S	Cr	Zn
				[%]			
1	13.7	56.10	0.04	0.29	0.15	0.035	0.0038
2	7.00	51.10	0.09	0.24	0.04	0.028	0.0036
3	8.27	55.98	0.11	0.22	0.016	0.040	0.0059
4	7.19	56.55	0.10	0.15	0.014	0.024	0.0061
5	11.6	55.51	0.03	0.43	0.013	0.038	0.018
6	9.50	58.14	0.03	0.05	0.006	0.040	0.052
7	5.54	57.80	0.15	0.44	0.014	0.010	0.0052

Table 2 Chemical analysis of tested sinter – part 2.

Sample	SiO_2	CaO	MgO	Al_2O_3	K_2O	TiO_2	P_2O_5
				[%]			
1	8.83	9.46	1.24	1.16	0.05	0.54	0.14
2	6.38	14.90	1.10	1.19	0.03	0.52	0.13
3	8.36	9.51	1.79	0.99	0.02	0.049	0.13
4	8.73	8.26	1.31	0.93	0.05	0.048	0.12
5	8.97	9.37	1.26	0.86	0.01	0.044	0.11
6	8.20	6.91	1.18	1.09	0.07	0.067	0.10
7	8.40	8.20	1.79	1.13	0.06	0.057	0.10

Table 4 Porosity and density of samples before reduction test.

Sample	ϕ [%]	ρ_s [g cm^{-3}]	ρ [g cm^{-3}]
1	9.55	4.62	3.65
2	9.82	4.21	3.71
3	6.61	4.42	3.70
4	6.46	4.16	3.76
5	7.26	4.18	3.77
6	7.86	4.39	3.74
7	5.81	4.28	3.82

Table 5 Porosity and density of samples after reduction test.

Sample	ϕ [%]	ρ_s [g cm^{-3}]	ρ [g cm^{-3}]
1	32.77	4.87	2.96
2	34.28	5.12	3.20
3	44.12	5.10	2.72
4	39.03	5.19	2.86
5	35.49	5.25	3.30
6	35.89	5.19	2.96
7	37.05	5.37	3.11

the product too sintered resulting in its hard reducibility. Creating of fayalite in the sinter during its production is possible to reduce by CaO or $CaCO_3$ forming silicates or ferrites at high temperatures instead of fayalite [22].

However, after the reduction at 950 °C the porosity of sample 2 was not retained so significant. The highest porosity after the reduction at 950 °C was indicated in sample 3.

These samples and the changes in their microstructures were studied through SEM analysis. In Figs. 3 and 4 are shown the representative pictures of surface structure of the virgin samples before reduction process. Sample 2 before reduction was created by wide fragments of ferrous elements and little undistinguished areas created mainly by oxygen accompanied by elements such as Na, Mg, Ca, and Si (Table 6). On the surface of sample 3 was detected higher ratio of Fe than on the surface of sample 2 (Table 7). After the reduction testing the surface of both samples (Figs. 5 and 6**)** was visibly noticeably transformed. The wide ferrous fragments were reduced into small formation. There were noticed fibrous areas created by oxygen and accompanying elements. Ferrous fragments on the surface of tested sample 2 and sample 3 were reduced and after their reduction there were detected elements such as O_2, Mg, Si, Ca, and Al (Tables 8 and 9). However, on

Table 6 Surface microanalysis of sample 2 before.

	O_2	Na	Mg	Al	Si	Ca	Fe
1a	42.52	–	–	0.48	0.12	0.19	56.69
2a	55.33	0.62	0.82	3.78	15.11	18.05	6.31

Table 7 Surface microanalysis of sample 3 before.

	O_2	Na	Mg	Al	Si	Ca	Fe
1a	22.73	–	–	0.28	0.28	0.36	76.35
2a	46.02	0.22	1.24	0.81	23.11	12.08	16.53

Table 8 Surface microanalysis of sample 2 after.

	O_2	Na	Mg	Al	Si	Ca	Fe
1	0.42	–	0.25	0.20	–	0.80	98.25
1	1.55	–	0.15	0.38	–	0.89	97.03
2	33.27	0.32	1.26	11.35	–	29.70	24.11
3	51.71	0.24	0.15	13.72	0.41	31.86	1.91

Table 9 Surface microanalysis of sample 3 after.

	O_2	Mg	Al	Si	Ca	Fe
1	5.57	1.66	1.43	0.60	2.04	88.70
1	3.83	0.65	1.06	0.47	1.42	92.57
2	46.85	0.68	0.48	13.26	32.56	6.17

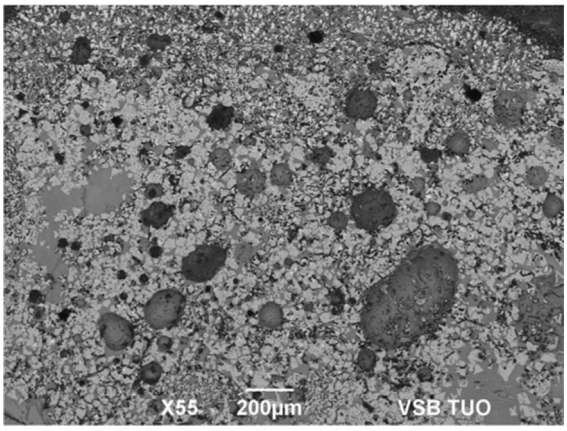

Figure 8 SEM on sample 2 after reduction.

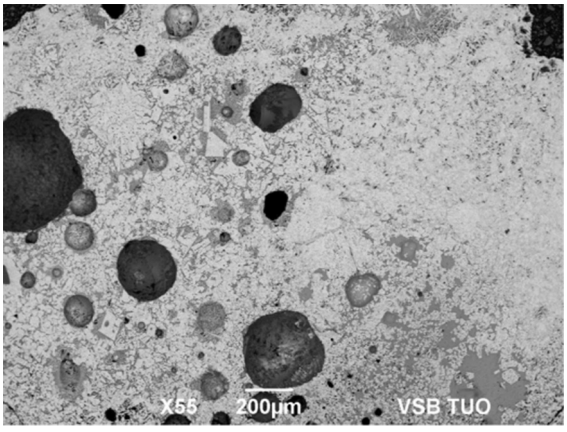

Figure 9 SEM on sample 3 before reduction.

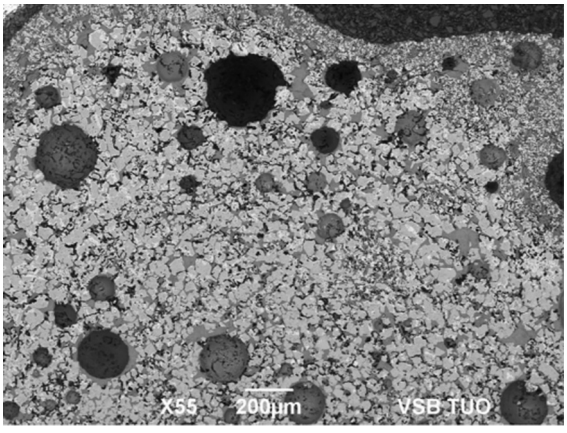

Figure 10 SEM on sample 3 after reduction.

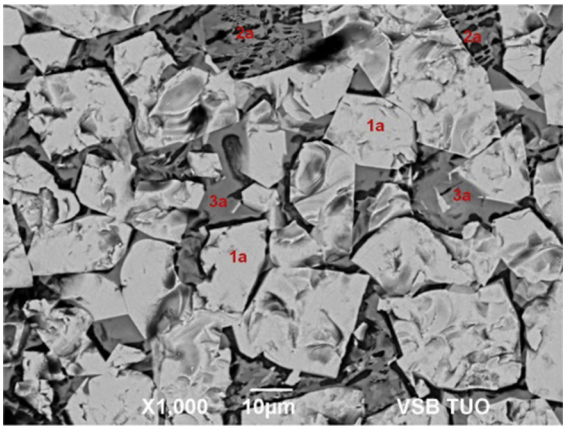

Figure 11 Margin of sample 2 before reduction.

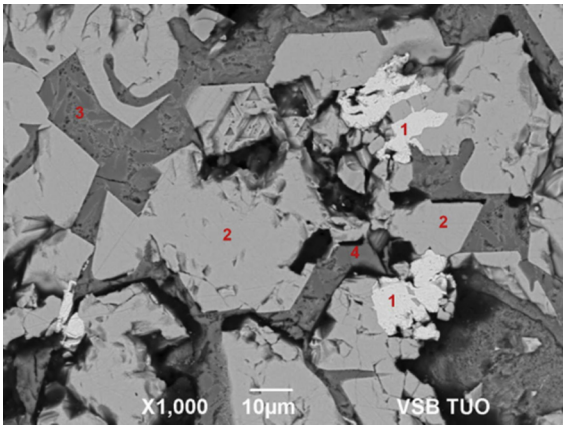

Figure 12 Margin of sample 2 after reduction.

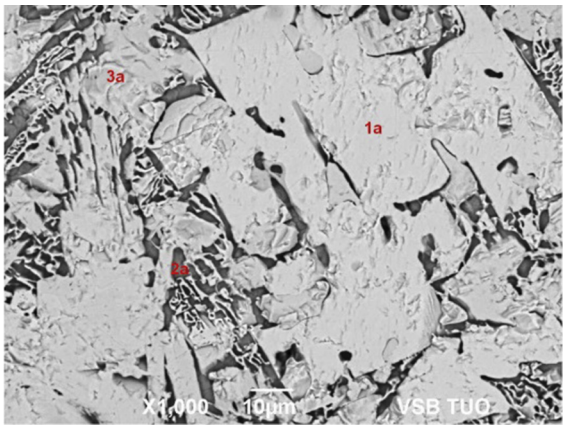

Figure 13 Margin of sample 3 before reduction.

surface of sample 3 was detected no Na as it is presented in Table 9. Figs. 7–10 present view of samples microstructure in higher magnitude. The analyses of margins of samples 2 and 3 before and after reduction are documented in Figs. 11–14 with detail information recorded in Tables 10–13. In margin structure of virgin samples were regions in which the presence of iron oxides was recorded. Some ferrous oxides contained elements such as Mg and Ca. There were identified higher content of Ca, Si oxides and trace amount of Fe and P. In the margin structure of samples 2 and 3 before reduction were

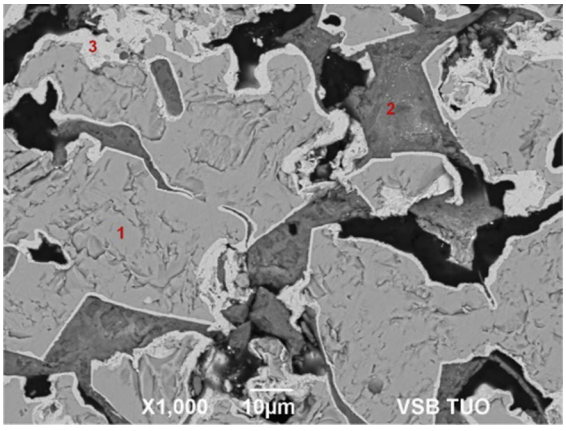

Figure 14 Margins of sample 3 after reduction.

observed sharp regions with ferrous oxides and Si and Ca. After 950 °C reduction in the samples 2 and 3 were identified porous elements of almost pure Fe and darker segments of Ca and Si oxides. There was noted metallic film on the large particles of Fe oxides in the margin structure of sample 3.

The statistical evaluation of acquired experimental results revealed rather a low correlation between porosity of tested samples and their reducibility (R = 0.426). The porosity of studied samples was affected by sample basicity (R = 0.747). A strong effect of FeO content on porosity of these samples was not confirmed. There was recorded a close relation between reducibility and true density of samples (R = 0.896), which was interpreted that the volume of any open and closed pores of studied metallurgical sinter had not affected the sample reducibility.

Table 10 Analysis of sample 2 before reduction.

	O_2	Mg	Al	Si	Ca	Fe
1a	36.20	2.87	0.47	–	0.96	59.51
1a	37.00	2.63	0.49	–	1.03	58.84
2a	45.20	0.47	1.17	14.38	21.63	17.15
2a	45.05	0.47	1.29	14.94	16.37	21.74
3a	47.58	0.42	1.26	17.49	23.84	9.42
3a	48.10	0.43	1.43	17.23	23.58	9.24

Table 11 Analysis of sample 2 after reduction.

	O_2	Mg	Al	Si	Ca	Fe
1	–	–	–	–	–	100
1	–	–	–	–	–	100
2	29.58	–	0.44	0.36	–	69.61
2	30.16	–	0.52	0.28	–	69.04
3	44.27	–	1.13	16.88	24.53	13.20
4	46.11	–	0.96	19.93	26.45	6.54

Table 12 Analysis of sample 3 before reduction.

	O_2	Na	Mg	Al	Si	Ca	Fe
1a	37.72	–	–	0.40	–	–	61.89
2a	57.56	0.28	0.28	1.37	16.40	18.97	5.14
3a	35.71	–	1.32	0.49	–	0.63	61.86

Table 13 Analysis of sample 3 after reduction.

	O_2	Mn	Mg	Al	Si	Ca	Fe
1	29.78	0.5	0.93	0.60	–	–	68.9
2	46.53	–	0.15	1.22	16.39	24.72	10.99
3	–	–	–	–	–	–	100

4. Conclusions

Industrial sinter sampled from a metallurgical company was subjected to a comprehensive set of characterizations on their basic structural properties toward their reducibility and processing in blast furnace feedstock. Several concluding remarks could be drawn as follows:

1. Porosity of tested sinter increased multiply at high temperature, whereas density of samples was not affected by temperature significantly.
2. Porosity of closed pores ranged from 5.1% to 9.82% and after reduction 32.77% to 44.12%. Density was measured in the range from 3.65 to 3.82 g cm^{-3} and for reduced samples from 4.87 to 5.37 g cm^{-3}.
3. The maximum porosity was measured in sample with the highest reducibility index and basicity. However, the set of samples did not prove significant statistical correlation between porosity and reducibility. There was confirmed the effect of sample basicity on their porosity. The study revealed a correlation between true density and reducibility of samples excluding the volume of any open and close pores. For verified conclusion the sample range will be extended in future work.
4. To visually compare the pore structure of virgin and reduced samples SEM analysis was carried out in combination with EDX to determine the element composition. In general, the pores of both samples include macro-pores or cavities with the size of millimeters and mesopores in the micrometer range. The images indicate the effect of high temperature on iron oxide reduction. After reducibility test in CO environment at 950 °C, high ratio of Fe in core of samples, in some points reaching 100%, was noted. The elemental analysis accompanying the images identified more complete reduction in sample 2 which was found to be the most porous virgin sample in the testing batch. SEM analysis proved the positive effect of higher porosity on reduction of sample.

Acknowledgments

This paper was conducted within the framework of the project LO1404: Sustainable development of ENET Centre and supported by Specific research SP2017/98 –Adjustment of synthesis gases for their utilization in secondary power machines.

References

[1] A. Babich, D. Senk, H.W. Gudenau, K.Th. Mavrommatis, Ironmaking, Department of ferrous Metallurgy at the RWTH Aachen University, Aachen, 2008.
[2] K. Nishioka, T. Murayama, Y. Ono, Estimation of effective thermal diffusivity of porous solid using data for image processing, ISIJ Int. 36 (2) (2015) 150–155.
[3] G. McCann, V. Strezov, J.A. Lucas, T. Evans, L. Strezov, Iron ore characterisation during high temperature thermal processing, Dev. Chem. Eng. Miner. Process 12 (3/4) (2004) 369–382.
[4] T. Aizawa, Y. Suwa, Meso-porous modelling for theoretical analysis of sinter ores by the phase-field unit-cell method, ISIJ Int. 45 (4) (2005) 587–593.
[5] M. Fröhlichova, R. Findorak, J. Legemza, Arch Metal Mater 58 (1) (2013) 179–185, http://dx.doi.org/10.2478/v10172-012-0170-9.
[6] Fu-You Tian, Lian-Feng Huand, Li-Wu Fan, Yuan-Kai Weng, Xiao-Yuan Ying, Zi-Tao Yu, Ke-Fe Cen, A comprehensive characterization on the structural and thermophysical properties of sintered ore particles toward waste heat recovery applications, Appl. Therm. Eng. 90 (2015) 1007–1014.
[7] O.S. Bölukbasi, B. Tufan, T. Batar, A. Altun, The influence of raw material composition on the quality of sinter, Nat. Sci. 1 (9) (2013) 37–47.
[8] J. Janowski, A. Sadowski, W. Kraj, T. Ratajczak, Determination of porosity of reduced hematite by stereologic methods, J. Mater. Sci. 33 (2) (1998) 477–486.
[9] V.I. Shatokha, Yu. Korobeynikov, L.V. Kamkina, N.A. Kolbin, Application of 3D tomography method for analysis of iron-ore sinter porosity. Part 2: Open and closed porosity characteristics, Metallurgical Min. Ind. 2 (6) (2010) 384–389.
[10] V. Shatokha, I. Korobeynikov, E. Maire, L. Gremillard, J. Adrien, Iron ore sinter porosity characterisation with application of 3D X-ray tomography, Ironmaking Steelmaking 37 (5) (2010) 313–319, http://dx.doi.org/10.1179/030192310X12683045805865.
[11] M.B. Hanel, H. Mali, J.F. Schenk, H. Stocker, M. Skorianz, Characterization of different lump ore brands according to industrial-scale process conditions by means of reducibility testing and morphological investigation, AISTech – Iron Steel Technol. Conf. Proc. 1 (2013) 447–456.
[12] A. Smolinski, D. Burchart-Korol, J. Korol, Chemometric study of sinter mixtures used in sinter plants in Poland, Metalurgija 54 (1) (2015) 98–100.
[13] Ram P. Bhagat et al, Effect of size parameters of mix ingredients on the porosity and reduction characteristics of sinter, Steel Res. Int. 78 (6) (2007) 451–454.
[14] A. Konstanciak, The effect of blast furnace coke quality on the possibility of its use, Metalurgija 52 (2) (2013) 193–196.
[15] P. Pustějovská, S. Jursová, Research on high temperature properties of iron ore materials, Acta Metallurgica Slovaca 20 (2) (2014) 135–139.
[16] ISO 4695:2007.
[17] S. Jasienska, A. Ledzki, J. Orewczyk, Contribution to the study of physico-chemical properties and composition of high basicity sinters Revue de metallurgie-cahiers d informations techniques. Vol. 93, 1996, No. 1. p. 43–53.
[18] Srinivas Dwarapudi et al, Effect of MgO in the form of magnesite on the quality and microstructure of hematite pellets, Int. J. Miner. Process. 112–113 (2012) 55–62.
[19] E.A. Mousa, Effect of basicity on wustite sinter reducibility under simulated blast furnace conditions, Ironmaking Steelmaking 41 (6) (2014) 418–429, http://dx.doi.org/10.1179/1743281213Y.0000000136.
[20] T. Maeda, Lim Bi, Y. Ono, Effects of basicity and porosity on the reducibility of iron-ore sinter, Trans. Iron Steel Inst Jpn. 24 (10) (1984), B332-B332.
[21] M. Bernasowski, Theoretical study of the hydrogen influence on iron oxides reduction at the blast furnace process, Steel Res. Int. 85 (4) (2014) 670–678.
[22] T. Amadevi, R. Sah, P.C. Mahapatra, Influence of sinter basicity (CaO, SiO_2) on low and high aluminia iron ore on sinter quality, Trans. Inst. Min. Metal., Section C: Miner. Process. Extractive Metall. 123 (2) (2014) 75–85.